LA-UR-84-3068

CONF-850133--1

Los Alamos National Laboratory is operated by the University of California for the United States Department of Energy under contract W-7405-ENG-36

TITLE INFLUENCE OF THE ATMOSPHERE ON REMOTELY SENSED REFLECTION FROM VEGETATION SURFACES

LA-UR--84-3068

DE85 000658

AUTHOR(S) C. Simmer, T-DOT
S.A.W. Gerstl, T-DOT

SUBMITTED TO Optical Society of America
Lake Tahoe, Nevada
January 15-18, 1985
Topical Meeting on Optical
Remote Sensing of the Atmosphere

MASTER

DISCLAIMER

Los Alamos Los Alamos National Laboratory
Los Alamos, New Mexico 87545

Influence of the Atmosphere On Remotely Sensed Reflection From Vegetation Surfaces

C. Simmer and S.A.W. Gerstl

Theoretical Division, Los Alamos National Laboratory
T-DOT, P.O. Box 1663, MS P27
Los Alamos, New Mexico 87545

ABSTRACT

Multiple scattering of solar radiation in a vegetation canopy is modelled equivalent to absorbing and scattering in a turbid medium with direction-dependent cross sections. Perturbations of plant reflection patterns due to atmospheric effects are computed at different altitudes and compared to the angular reflection characteristics caused by Lambertian surfaces of varying albedoes.

INFLUENCE OF THE ATMOSPHERE ON REMOTELY SENSED REFLECTION FROM VEGETATION SURFACES

C. Simmer and S.A.W. Gerstl

Theoretical Division, Los Alamos National Laboratory,
T-DOT, MS P371, Los Alamos, New Mexico 87545

Introduction

One purpose of vegetation canopy modelling is to predict the solar radiation reflection distribution produced by the canopy, in order to use it as an identifier in remote sensing. For remote sensing by satellite or aircraft the measured reflectance pattern also contains the signature of the atmosphere, which changes both the radiation distribution of the downwelling solar source before it reaches the canopy, as well as the reflected upwelling signal before it reaches the sensor.

The theory underlying these calculations is described in detail by Gerstl and Zardecki.[1] Solar radiative transfer through a coupled system of atmosphere and plant canopy is modelled as a multiple scattering problem through a layered medium of random scatters. The radiative transfer equation is numerically solved by the discrete-ordinates finite-element method. For the atmosphere we used the optical data of Shettle and Fenn.[2] Analytic expressions are derived which allow the calculation of scattering and absorption cross-sections for any plant canopy layer from measurable biophysical parameters such as the Leaf Area Index (LAI), the radiation interception per leaf $G(z,\underline{\Omega})$ with $\underline{\Omega}$ the direction of the incoming radiation, and the individual leaf hemispheric reflectance and transmittance ρ and τ. Using these parameters, the canopy volume scattering and absorption coefficients, σ^o_s and σ_a, per canopy layer of thickness Δ(cm), are expressed as

$$\sigma^o_s(z,\lambda,\underline{\Omega}) = [\rho(\lambda) + \tau(\lambda)] \cdot G(z,\underline{\Omega}) \frac{LAI(z)}{\Delta} ,$$

and

$$\sigma_a(z,\lambda,\underline{\Omega}) = [1-\rho(\lambda) - \tau(\lambda)] \cdot G(z,\underline{\Omega}) \frac{LAI(z)}{\Delta} .$$

λ and z indicate the wavelength and the vertical coordinates, respectively. A simple expression for the canopy structure-dependent G-function, first introduced by Ross[3], is derived following Suits[4] by replacing individual leaves with their horizontal (H) and vertical (V) projections. We obtain the following expressions for the direct and scattered radiation $G_o(z)$ and $G_s(z)$, respectively:

$$G_s(z) = \frac{1}{2} ,$$

$$G_o(z) = \frac{H}{H+V} \cdot \cos\theta_o + \frac{2V}{\pi(H+V)} \cdot \sin\theta_o .$$

Here θ_o indicates the solar zenith angle. Although a general expression to derive a scattering phase function P for a canopy from the phase function of the individual leaf and the leaf angle distribution is given by Ross[3], we assume isotropic scattering for these calculations, because neither the scattering phase function of individual leaves nor the leaf angle distributions are known accurately enough to date to perform a reliable determination of P.

Results

Figures 1a and 1b show the upwelling radiance distributions produced by two different Lambertian reflectors at different altitudes. The lowest surface in the figures gives the upward radiance at ground level, which is a horizontal plane due to the definition of a Lambertian reflector. The middle and upper planes refer to the upward radiance distributions at 1-km and 70-km, respectively. Both calculations were carried out for a solar-zenith angle of 30° and for a wavelength of 0.55 μm. Viewing zenith, θv, and azimuth angles, ϕv, are plotted relative to the principal plane (sun at $\phi v = 180^{\circ}$). Figure 1a shows the results for a 100% Lambertian reflector and Fig. 1b for a 20% Lambertian reflector. The plots show clearly that even Lambertian surfaces produce radiance patterns already at 1-km height, which are quite different from a Lambertian distribution. Although the pattern remains symmetric with respect to the principal plane ($\phi v = 0^{\circ}$ and $\phi v = 180^{\circ}$), there is for both cases an increasing azimuthal dependency with increasing view zenith angle. For a surface albedo of 100%, the radiance pattern, however, remains rather flat for view zenith angles up to 60°. For higher zenith angles, the radiance decreases by about 20% caused by increased atmospheric extinction due to the increased path length. (Compare Fig. 1a.) Note that all radiance values for $\theta v > 80^{\circ}$ are set constant because we did not correct our results for the curvature of the Earth's surface. While the radiance pattern for this case is dominated by the strong uniform illumination from the surface, in the second case (albedo 20%), the back and side scattering properties of the atmosphere become more prominent resulting in an increased angular dependency at higher altitudes. (Compare Fig. 1b.) Viewing with the sun direction ($\theta v = 30^{\circ}$, $\phi v = 180^{\circ}$ indicated by ✦), we observe a localized minimum, while viewing from opposite to the sun ($\theta v = 30^{\circ}$, $\phi v = 0^{\circ}$, indicated by ○) an extended region of low radiance values is found. For large view zenith angles ($\theta v > 60^{\circ}$), we find just the opposite: higher values in the principal plane and lower values inbetween. Comparing Figs. 1a and 1b at large view zenith angles ($\theta v > 60^{\circ}$) confirms the conclusions by Fraser and Kaufman[4], that for high surface albedoes (bright surfaces) the upwelling radiance at higher altitudes is reduced compared to the surface values, while for low surface albedoes (darker surfaces) the atmospheric effect increases the upwelling radiance.

Figures 2a and 2b show for the wavelength 0.55 μm and 0.85 μm, respectively the radiance patterns produced by our combined canopy-atmosphere model. The lowest plane in the figures now refers to the radiance distribution directly above the canopy. The canopy modelled is a soybean canopy with a measured LAI vertical profile and hemispheric transmission and reflection coefficients from Ranson, et. al.[5] The radiance pattern directly above the canopy shows for both wavelengths the typical "bowl shape" as measured by Kimes and Deering[6]: a minimum (although shallow for $\lambda = 0.55$ μm) at near-nadir zenith angles and increasing radiance values with increasing zenith angle, as marked by heavy lines in Figs. 2a and 2b. The distributions are independent of the azimuth angle because we assumed isotropic scattering within the canopy combined with a Lambertian soil albedo (20%). The "bowl shape" is much more pronounced in the near-infrared than in the visible and increases with increasing solar zenith angle (not shown here). The bowl shape of canopy reflectance is often assigned to shading between canopy elements[7,8] but it should be pointed out that shading is not included in our present canopy model. This indicates that the absorption and scattering properties of the individual leaves also contribute to this shape. However, the radiation transport through the

atmosphere changes these reflectance patterns significantly. In the visible region, the bowl-shape disappears almost completely already at 1-km altitude, and the pattern of 70-km altitude is almost identical to the radiance distribution at the same height over the 20% Lambertian reflector (Fig. 1b). The bowl shape changes into a "saddle shape" due to atmospheric effects. In the near-infrared, where the bowl-shape is much more pronounced and scattering increases the total spectral albedo to almost 50%, the bowl shape may still be recognized at 1-km and at 70-km altitudes. However, the increase of radiance for high view zenith angles ($\theta v > 60^{o}$) at the top of the canopy is overcompensated by the increased absorption due to the longer path length at the top of the atmosphere, as demonstrated in Fig. 1a.

Conclusion

If the angular distribution of the radiance emerging from the top of the atmosphere is used for the remote sensing of vegetative canopies, it is more appropriate to use spectral bands in which canopies show high reflection and low absorption, namely, the near-infrared, and not the visible. Remote sensing in the visible part of the spectrum where absorption is dominant within the canopy suffers from strong perturbations by atmospheric effects. However, measured angular reflectance distributions directly above orchard grass and soybeans show a more pronounced bowl shape than we obtained from our canopy model. Preliminary data indicate that these more pronounced reflectance patterns may still be observable above the atmosphere despite the atmospheric perturbations described in the present analysis.

References

1. S.A.W. Gerstl and A. Zardecki, "A Coupled Atmosphere/Canopy Model for Remote Sensing of Plant Reflection Features," in press, Appl. Opt. (1984).
2. E.P. Shettle and R.W. Fenn, Air Force Geophysics Laboratory report AFGL-TR-79-0214 (Sept. 1979).
3. J. Ross, The Radiation Regime and Architecture of Plant Stands, Dr. W. Junk Publ., The Hague-Boston-London (1981).
4. R.S. Fraser and Y.J. Kaufman, Am. Meterological Soc. Proc. Fifth Conf. Atmos. Rad., Oct. 31- Nov. 4, 1983, pp. 98-102.
5. K.J. Ranson, et al., AGRISTARS Tech. Report SR-P2-04278 (NAS9-15466), 1982.
6. D. Kimes and D. Deering, NASA Tech. Memorandum 86078, R.E. Murphy and D. Deering (Eds.), pp. 75-86, March 1984.
7. K.T. Kriebel, Appl. Opt. 17,2, pp. 253-259 (June 1978).
8. D.S. Kimes, J.Opt.Soc. Am. A, 1, pp. 725-737 (July 1984).

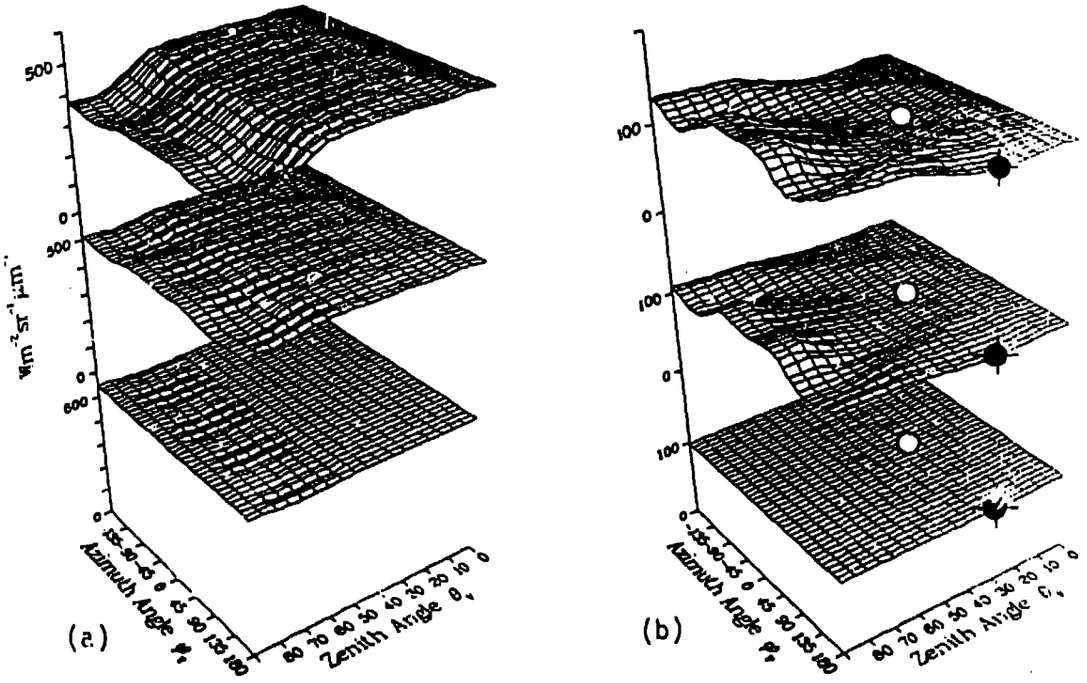

Fig. 1. Computed upwelling radiance distribution for λ = 0.55-μm at altitudes 0,1 and 70-km above a 100% (a) and 20% (b) Lambertian reflector.

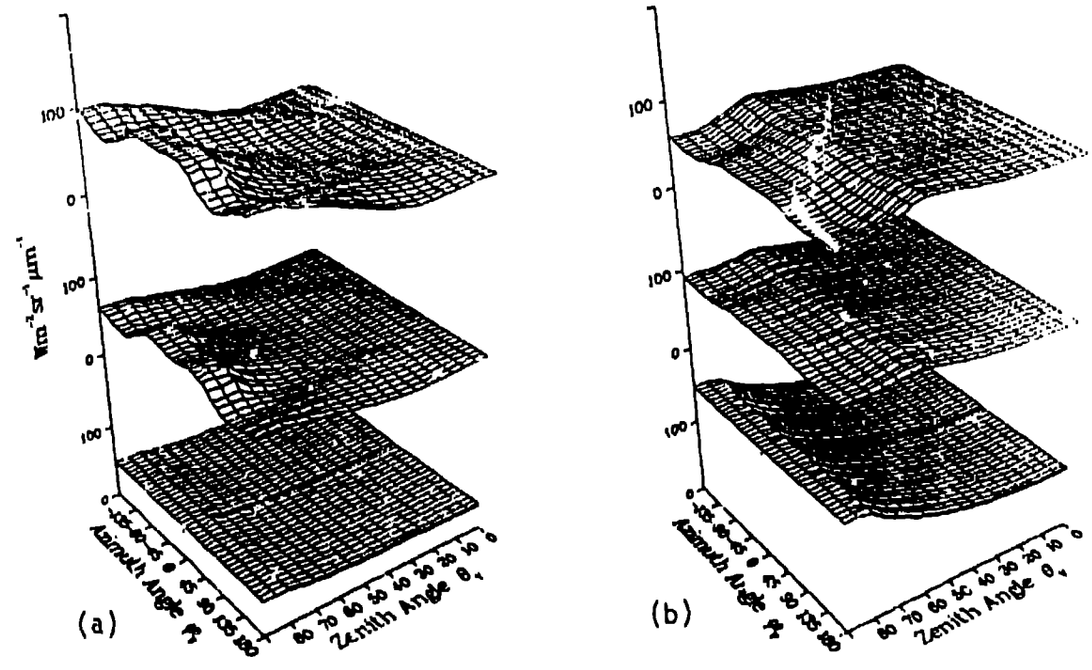

Fig. 2. Computed upwelling radiance distribution for λ = 0.55-μm (a) and λ = 0.85-μm (b) above a modelled soybean canopy of LAI = 1.0. All computations assume a rural atmosphere model with aerosol optical depth of 0.1 at 0.55 μm, corresponding to a surface visual range of 50-km.